Biochimica et Biophysica Acta 1797 (2010) 1389–1397

Contents lists available at ScienceDirect

Biochimica et Biophysica Acta

journal homepage: www.elsevier.com/locate/bbabio

Absence of uncoupling protein-3 leads to greater activation of an adenine nucleotide translocase-mediated proton conductance in skeletal muscle mitochondria from calorie restricted mice

Lisa Bevilacqua [1], Erin L. Seifert [1], Carmen Estey [1], Martin F. Gerrits, Mary-Ellen Harper *

Department of Biochemistry, Microbiology and Immunology, Faculty of Medicine, University of Ottawa, Ottawa, Ontario, Canada KIH 8M5

ARTICLE INFO

Article history:
Received 24 July 2009
Received in revised form 15 January 2010
Accepted 17 February 2010
Available online 3 March 2010

Keywords:
Aging
Calorie restriction
Mitochondrial uncoupling
Proton leak
Oxidative stress
Indirect calorimetry
Rodent models of aging
Bongkrekate

ABSTRACT

Calorie restriction (CR), without malnutrition, consistently increases lifespan in all species tested, and reduces age-associated pathologies in mammals. Alterations in mitochondrial content and function are thought to underlie some of the effects of CR. Previously, we reported that rats subjected to variable durations of 40% CR demonstrated a rapid and sustained decrease in maximal leak-dependent respiration in skeletal muscle mitochondria. This was accompanied by decreased mitochondrial reactive oxygen species generation and increased uncoupling protein-3 protein (UCP3) expression. The aim of the present study was to determine the contribution of UCP3, as well as the adenine nucleotide translocase to these functional changes in skeletal muscle mitochondria. Consistent with previous findings in rats, short-term CR (2 weeks) in wild-type (Wt) mice resulted in a lowering of the maximal leak-dependent respiration in skeletal muscle mitochondria, without any change in proton conductance. In contrast, skeletal muscle mitochondria from *Ucp3*-knockout (KO) mice similarly subjected to short-term CR showed no change in maximal leak-dependent respiration, but displayed an increased proton conductance. Determination of ANT activity (by measurement of inhibitor-sensitive leak) and protein expression revealed that the increased proton conductance in mitochondria from CR *Ucp3*-KO mice could be entirely attributed to a greater acute activation of ANT. These observations implicate UCP3 in CR-induced mitochondrial remodeling. Specifically, they imply the potential for an interaction, or some degree of functional redundancy, between UCP3 and ANT, and also suggest that UCP3 can minimize the induction of the ANT-mediated 'energy-wasting' process during CR.

1. Introduction

Calorie restriction (CR) without malnutrition markedly and consistently increases lifespan in all species tested, and reduces age-associated pathologies in mammals (for review: [1]) including age-related biomarkers in humans [2]. It is thus of interest to determine the mechanisms by which CR modifies organismal physiology. A phenotype consistently associated with CR is a reduction in oxidative stress [3–5]. This reduction in oxidative stress with CR is consistent with a central theory of aging which proposes that the age-related loss of physiological function is due to the progressive accumulation of oxidative damage to macromolecules [6–8]. Mitochondria are the major cellular source of reactive oxygen species (ROS) that contribute to oxidative damage, and ~0.1–2% of the O_2 consumed by the respiratory chain results in ROS generation [9,10]. Indeed, alterations in mitochondrial content and function are thought to underlie some of effects of CR [11]. Consistent with this notion are observations in various cell types of a remodeling of the mitochondrial mass [4,12–17].

We have been interested in CR-induced mitochondrial remodeling in skeletal muscle, and specifically in H^+ leak-dependent mechanisms that lower ROS production. Mitochondria, including mitochondria in human muscle [18], express a non-phosphorylating component of O_2 consumption that is mediated by H^+ return to the mitochondrial matrix via mechanisms other than the ATP synthase [19]. The physiological significance of this H^+ leak may be to offset excess nutrient intake and to mitigate oxidative stress [20,21]. In skeletal muscle mitochondria, ~50% of the H^+ leak is attributed to the adenine nucleotide translocase (ANT) much of which is not inhibited by the specific inhibitor carboxyatractylate (CAT) and thus is not due to ADP/ATP exchange or to ANT activation [22]; this CAT-insensitive component is termed 'basal leak' [22]. ANT can also catalyze a CAT-inhibited inducible H^+ leak; activators are fatty acids [22–25], alkenals [26] and AMP [27]. In skeletal muscle, uncoupling protein-3 (UCP3), a mitochondrial inner membrane protein with homology to the prototypical uncoupling protein, UCP1, can also be activated by fatty acids and alkenals [28,29]. UCP3 has been associated with

* Corresponding author. Tel.: +1 613 562 5800x8235; fax: +1 613 562 5452.
E-mail address: Maryellen.harper@uottawa.ca (M.-E. Harper).
[1] These authors contributed equally to this work.

0005-2728/$ – see front matter © 2010 Elsevier B.V. All rights reserved.
doi:10.1016/j.bbabio.2010.02.018

lowered oxidative stress; one model proposes 'mild uncoupling' (*i.e.*, increased H^+ leak) as the mechanism [28]. Thus, modulation of H^+ leak, an energy inefficient but protective process, by CR could have significant cellular and organismal consequences.

We reported previously that rats subjected to 40% CR of variable duration (2-wks, 12 or 18 months) demonstrated a rapid and sustained decrease in maximal leak-dependent respiration in skeletal muscle mitochondria [4,15]. This was accompanied by lower mitochondrial ROS generation and oxidative stress, and increased UCP3 protein content. We hypothesized therein that UCP3 was involved. The aim of the present study was to determine the contribution of UCP3 to these CR-induced functional changes in skeletal muscle mitochondria, utilizing UCP3 knockout mice (*Ucp3*-KO) and their wild-type (Wt) counterparts. Because of the important contribution of ANT to leak-dependent respiration, we also conducted studies in the presence and absence of CAT to delineate genotype and CR-induced changes in ANT-mediated leak.

2. Experimental procedures

2.1. Treatment of animals

Two-month old male C57BL/6J wild-type (Wt) and *Ucp3*-knockout (*Ucp3*-KO) mice were housed individually from weaning, with free access to water and rodent chow (5% fat by weight; Harlan 2018). The *Ucp3*-KO mice used in this study were backcrossed for 10 generations onto a C57BL/6J background. In all mice starting at 2 months of age, individual daily *ad libitum* food intake was measured over a two-week period to determine the amount of food required during the CR phase of the study. Mice were randomly assigned to control or CR treatment groups. The control mice were restricted to 95% of *ad libitum* intake to prevent the development of obesity. The CR mice were provided with a modified AIN-93M diet (Research Diets, New Brunswick, NJ) at 60% of *ad libitum* food intake. The energy intakes were 11.6 kcal/day for the control and 7.1 kcal/day for the CR mice. Throughout the study all animals were allowed free access to water, and were kept at 23 °C with lights on 0700–1900. Mice were cared for in accordance with the principles and guidelines of the Canadian Council on Animal Care and the Institute of Laboratory Animal Resources (National Research Council). The Animal Care Committee of the University of Ottawa approved the study.

2.2. Organ weight measurements

Tissues (heart, kidney, liver, and epididymal white adipose tissue (EWAT)) were removed immediately after the mice were sacrificed, blotted dry, then weighed.

2.3. Indirect calorimetry

Whole-body oxygen consumption and respiratory exchange ratios (RER) were measured using a four-chamber Oxymax open-circuit indirect calorimeter with automatic temperature and light controls (Columbus Instruments, Columbus, OH). System settings included an airflow rate of 0.5 L/min, a sample line-purge time of 2 min, and a measurement period of 60 s every 12 min. Two days prior to sacrifice, mice were placed individually into the 2.5 L respiration chambers. Data were collected over a 24-hour period with the temperature maintained at 24 °C and with lights on from 0700 to 1900. The RER was calculated as the ratio of carbon dioxide production (VO_2) to O_2 consumption (VO_2). Data from each mouse were analyzed by the percent relative cumulative frequency (PRCF) procedure [30].

2.4. Isolation of skeletal muscle mitochondria

Skeletal muscle mitochondria were isolated from the hind limbs using a protocol adapted from [31,32]. All procedures were performed on ice. Freshly dissected muscle was placed in ice-cold basic medium (BM: 140 mM KCl, 20 mM HEPES, 5 mM $MgCl_2$, 1 mM EGTA, pH 7.0). Connective and adipose tissues were removed. The skeletal muscle was blotted dry then weighed, then minced finely for 2 min on a Teflon cutting board, on ice. The minced muscle was suspended in 5 volumes of homogenization medium (HM: BM plus 1 mM EGTA, 1 mM di-potassium ATP, and 1% w/v defatted BSA, pH 7.0). Subtilisin A (Type VIII, Sigma) was added (2 U/g) and the suspension was swirled constantly for 2 min on ice. The muscle suspension was then diluted 6-fold with subtilisin A-free HM and centrifuged at $9681 \times g$ for 10 min. Protease-containing supernatant was discarded and the pellet was resuspended in fresh HM and homogenized at ~350 RPM, twice with a loose- (TC = 300 μm) and twice with a medium- (TC = 120 μm) fitting Teflon pestle using a Potter-Elvehjem-type homogenizer. The homogenate was centrifuged at $484 \times g$ for 10 min. The supernatant was retained and centrifuged at $9681 \times g$ for 10 min. The resulting crude mitochondrial pellet was resuspended in BM containing 1% w/v BSA, then incubated for 10 min to permit myofibrillar repolymerization. Residual myofibrillar material was pelleted at $484 \times g$. The supernatant was retained and centrifuged at $9681 \times g$ for 10 min. The mitochondrial pellet was washed once in BM, and the final pellet was resuspended in 250–300 μl of BM. Protein concentration was determined using a modified Lowry assay, with BSA as the standard.

2.5. Measurement of mitochondrial H^+ leak kinetics

Oxygen consumption was measured in isolated skeletal muscle mitochondria (0.5 mg/ml) using a Hansatech Clark-type oxygen electrode (Norfolk, UK). Measurements were made in incubation medium (120 mM KCl, 5 mM HEPES, 5 mM $MgCl_2$, 1 mM EGTA, 5 mM KH_2PO_4, 0.3% defatted BSA, pH 7.4), at 37 °C. Proton leak measurements were conducted using succinate (10 mM) as the substrate, and carried out in the presence of nigericin (0.4 μg/ml), rotenone (5 μM), oligomycin (8 μg/mg protein), and incremental additions of malonate (10 mM, final concentration).

A methyltriphenylphosphonium ($TPMP^+$)-sensitive electrode was used to assess mitochondrial protonmotive force (PMF) in parallel with proton leak. The electrode was constructed as previously described [33]. The PMF comprises a voltage gradient due to charge separation and a pH (chemical) gradient. Nigericin (0.4 μg/ml), which transports K^+ out of the matrix in exchange for H^+, was added to dissipate the pH component of PMF. Since electrochemical equilibrium is achieved when the pH gradient has been dissipated, nigericin-mediated movement of K^+ creates a voltage gradient that is equal to the potential that had been stored as a pH gradient. A $TPMP^+$ standard curve was always generated prior to the initiation of respiration and membrane potential determinations. For standardization, 1 μM changes in $TPMP^+$ concentration were made to achieve a final $TPMP^+$ concentration of 5 μM. The Nernst equation was used to calculate membrane potential as previously described [34]. In a subset of experiments utilizing bongkrekic acid, PMF was determined fluorimetrically using 5 μM safranin [35].

To assess the role of the adenine nucleotide translocase (ANT) in H^+ leak, measurements of membrane potential and O_2 consumption were also conducted in the presence of 10 μM carboxyatractylate (CAT), or of 2 μM bongkrekic acid (BKA). CAT stabilizes ANT in the C conformation whereas BKA stabilizes ANT in the M conformation. For experiments utilizing BKA and their non-BKA controls, BSA and $MgCl_2$ were omitted from the incubation medium; BSA can bind BKA [36] and Mg^{2+} can inhibit leak processes [37]. To optimize binding of BKA to ANT, 2 μM ADP

was added ~3 min following bongkrekic acid addition [38], followed by succinate and oligomycin additions.

2.6. Measurement of mitochondrial ROS production

H_2O_2 emission rate was assayed as an index of superoxide production, using the p-hydroxyphenyl acetic acid (PHPA)/horseradish peroxidase (HRPO) assay [39]. H_2O_2 was detected fluorimetrically (excitation: 320 nm; emission: 400 nm) using a temperature-controlled microplate reader (Biotek, FLx 800). Assays were conducted as follows. Incubation medium (IM: 120 mM KCl, 5 mM HEPES, 5 mM $MgCl_2$, 1 mM EGTA, 5 mM KH_2PO_4 and 0.3% BSA (w/v); pH 7.4) was warmed for 10 min at 37 °C. Then PHPA (167 μg/mL), HRPO (9 U/mL), SOD (20 U/0.3 mL), and isolated mitochondria (0.3 mg/ml) were added to each well. Depending on the experimental conditions, the following were also added: malate (5 mM), antimycin A (5 μM), rotenone (5 μM), and oligomycin (8 μg/ml). The reaction was initiated by addition of substrate (succinate (10 mM), pyruvate/malate (10 mM/5 mM) or palmitoylcarnitine (18 μM)). H_2O_2 formation was followed as the increase in fluorescence. Each condition was assayed in duplicate, over 20–25 min, taking a fluorescence reading every 1 min. H_2O_2 production was determined as nmol H_2O_2/min/mg mitochondria using a standard curve generated in the presence of mitochondria.

2.7. Western blotting for UCP3 and ANT

Fifteen micrograms of mitochondrial protein were loaded into each lane of a Bio-Rad minigel system. A rabbit polyclonal primary antibody raised against human UCP3 (ab3477; AbCam) was used at 1:1000. The primary antibody for ANT (sc-9299; Santa Cruz Biotechnology) recognizes ANT1 and ANT2 and was used at 1:4000. The appropriate secondary antibody (donkey anti-goat IgG, goat anti-rabbit IgG; Santa Cruz Biotechnology) was diluted 1:2000 in PBS containing 5% (w/v) skim milk powder. Protein was detected by enhanced chemiluminescence (Amersham Pharmacia; Baie d'Urfe, Canada) and visualized using a Typhoon imaging system (Typhoon Trio, GE Healthcare). Protein bands and Coomassie-stained gels were quantified by densitometry (ImageJ). For each sample, the protein value was normalized to the value from the respective lane on the Coomassie-stained gel.

2.8. Statistical analysis

Comparisons between groups and genotypes were made by two-way ANOVA (independent samples) followed by Bonferroni post hoc contrasts where appropriate (Prism 4.l Graph Pad, San Diego, CA). Statistical significance was defined as $P<0.05$. All results are presented as mean ± standard error of the mean (SEM).

3. Results

3.1. Body and organ weights

The 2 wk CR intervention resulted in a ~20% reduction in body weight (BW) in both Wt and *Ucp3*-KO mice ($P<0.001$, pre-CR BW *vs.* BW after 2-wk CR), or a ~25% reduction in BW when compared to fed controls ($P<0.001$) (Table 1).

Weights of the respective organs (liver, heart, kidneys, and EWAT) were similar in control Wt and *Ucp3*-KO mice (Table 1). Two-wk CR resulted in a decrease in the absolute weight of all of these organs. However, as a proportion of BW, liver and kidney weights were unchanged (~3.8% and ~1.2% of BW, respectively), whereas heart weight increased from ~0.52% to 0.70% of BW ($P=0.008$), and EWAT decreased from 2.7% to 1.5% of BW ($P<0.001$). Thus, body composition changed with CR. These changes were similar in Wt and *Ucp3*-KO mice.

3.2. Whole-body energetics

Whole-body oxygen consumption (VO_2) and respiratory exchange ratio (RER) were determined in control and 2-wk CR Wt and *Ucp3*-KO mice by indirect calorimetry. Data are plotted as the percent relative cumulative frequency distribution, a quantitative approach enabling the detection of small differences in large data sets [30]. Whole-body VO_2 was similar in control Wt and *Ucp3*-KO mice (Fig. 1A), consistent with our earlier findings [40,41]. On a per mouse basis, 2-wk CR decreased whole-body VO_2 in both genotypes, and did so by a similar extent (20–25% reduction; Fig. 1A); mean daily values in ml/min/mouse were 1.60 ± 0.07 and 1.29 ± 0.09 for Wt control and CR mice respectively, and 1.56 ± 0.04 and 1.15 ± 0.05 for *Ucp3*-KO control and CR mice, respectively ($P<0.001$, control *vs.* CR).

Commonly, whole-body VO_2 is expressed per BW. When this was done, differences between control and CR mice disappeared (Fig. 1B). Mean mass-adjusted daily VO_2 for Wt control and CR mice was, respectively, 0.058 ± 0.001 and 0.057 ± 0.005 ml/min/g. Values for *Ucp3*-KO control and CR mice were, respectively, 0.055 ± 0.001 and 0.051 ± 0.003 ml/min/g. However, body composition changed with CR such that fat mass/BW decreased, heart mass/BW slightly increased, and liver and kidney mass/BW each stayed approximately the same (see Table 1). We and others have also found that muscle mass/BW remains similar or increases with CR [[2,42,43], Estey et al., in preparation]. Consequently, the proportion of lean tissue mass increases with CR, and VO_2 per lean tissue mass would thus be reduced with CR.

RER was similar in control Wt and *Ucp3*-KO mice (Fig. 1C); mean daily values were 0.870 ± 0.038 and 0.826 ± 0.018, respectively. CR was associated with a significant reduction in the mean daily RER, indicating increased oxidation of fatty acids. The reduction in RER was quantitatively similar in Wt and *Ucp3*-KO mice; mean daily RER values were 0.783 ± 0.025 for Wt CR and 0.789 ± 0.027 for *Ucp3*-KO CR mice ($P=0.008$, control *vs.* CR; two-way ANOVA).

3.3. H_2O_2 emission rate in isolated skeletal muscle mitochondria

Because CR has been associated with a reduction in ROS generation and oxidative stress [3–5,15], ROS production was determined in skeletal muscle mitochondria from control and CR Wt and *Ucp3*-KO mice. The mitochondrial ROS load was measured as the H_2O_2 emission rate. Different inhibitors and substrates were utilized to assess ROS formation due to electron leak at different sites in the mitochondrial electron transport chain. Pyruvate/malate and rotenone were used to

Table 1
Body and organ weights from wild-type (Wt) and Ucp3-KO mice, either subjected to 2 wk of 40% calorie restriction (CR), or not (CON).

	Wt CON	Wt CR	% Diff (control vs. CR)	*Ucp3*-KO CON	*Ucp3*-KO CR	% Diff (control vs. CR)
Initial body weight (g)	26.2 ± 0.37	26.5 ± 0.56		26.8 ± 0.64	26.1 ± 0.56	
Final body weight (g)	28.4 ± 0.51	21.2 ± 1.4	−25.3% ***	28.8 ± 0.5	21.1 ± 0.5	−26.7% ***
Liver (g)	1.12 ± 0.05	0.80 ± 0.03	−28.3% ***	1.05 ± 0.04	0.70 ± 0.04	−32.7%***
Heart (g)	0.16 ± 0.01	0.15 ± 0.01	−5.06%	0.15 ± 0.01	0.14 ± 0.01	−9.67%
Kidney (g)	0.30 ± 0.01	0.26 ± 0.01	−13.8%	0.33 ± 0.01	0.26 ± 0.01	−19.9% **
EWAT (g)	0.78 ± 0.07	0. 32 ± 0.06	−58.0% ***	0.75 ± 0.05	0.30 ± 0.03	−60.2% ***

Values are mean ± SEM, $n=6$/group. **$P=0.004$; ***$P<0.001$; two-way ANOVA, significant main effect of diet.

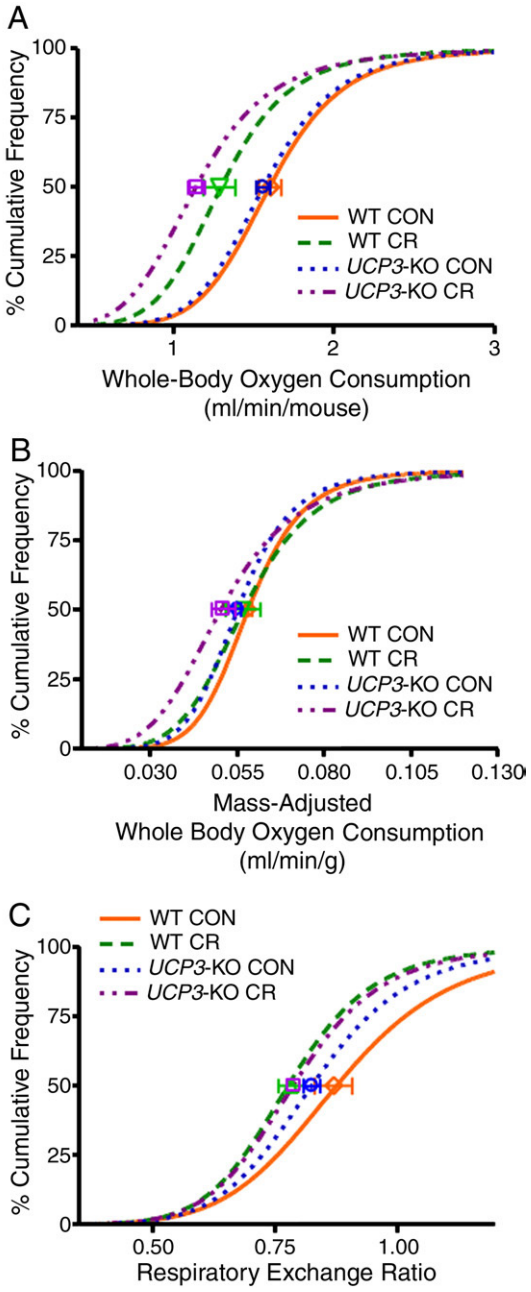

Fig. 1. Effect of 2-wk CR on whole-body energetics of Wt and *Ucp3*-KO mice. Whole-body oxygen consumption (VO_2) and respiratory exchange ratio (RER) were measured by indirect calorimetry. Data were analyzed using the percent relative cumulative frequency procedure [30]. (A) VO_2 per mouse was decreased following 2-wk CR to a similar extent in wild-type (WT) and *Ucp3*-KO mice, as compared to pair-fed control mice (CON). (B) Normalization of VO_2 to body weight resulted in similar VO2/g in CR and CON mice of each genotype. (C) RER was decreased following 2-wk CR to a similar extent in wild-type (WT) and *Ucp3*-KO mice, as compared to pair-fed CON mice. In each panel, symbols correspond to the median value ± SEM; diamonds: Wt CON, squares: Wt CR, circles: *Ucp3*-KO CON, triangles: *Ucp3*-KO CR; $n = 6$ mice/group. See text for further details concerning results from all panels.

assess ROS formation at complex I as well as at upstream sites such as the α-ketoglutarate dehydrogenase complex [44]. Fatty acid substrate (palmitoylcarnitine) and antimycin were used to determine ROS generation at complex III as well as at upstream sites such as the electron transfer flavoprotein (ETF) and ETF-ubiquinone oxidoreductase [45,46]. Use of succinate in the absence of inhibitors assessed ROS formation due to electron backflow through complex I [47], which depends on a high membrane potential. As shown in Table 2, there were no significant differences in H_2O_2 emission rate between control

Table 2
H_2O_2 emission rates in skeletal muscle mitochondria from wild-type (wt) and *Ucp3*-KO mice, subjected to 2-wk of 40% calorie restriction (CR), or not (CON).

	Wt CON	Wt CR	*Ucp3*-KO CON	*Ucp3*-KO CR
PCarn + Oligo + SOD	0.048 ± 0.005	0.058 ± 0.008	0.054 ± 0.012	0.072 ± 0.0086
PCarn + Anti + SOD	2.01 ± 0.34	1.61 ± 0.27	2.49 ± 0.53	1.79 ± 0.22
Succ + Rot + Anti + SOD	0.49 ± 0.07	0.46 ± 0.06	0.68 ± 0.14	0.58 ± 0.07
Succ	0.66 ± 0.06	0.66 ± 0.05	0.51 ± 0.11	0.72 ± 0.08
P/M + Rot + SOD	0.16 ± 0.01	0.18 ± 0.01	0.20 ± 0.03	0.23 ± 0.02

PCarn: palmitoylcarnitine (18 μM); Oligo: oligomycin (8 μg/ml); SOD: superoxide dismutase (20 U/ml); Anti: antimycin (5 μM); Succ: succinate (10 mM); Rot: rotenone (5 μM); P/M: pyruvates/malate (10 mM/5mM); Values are mean ± SEM, $n = 4$–6/group. $P > 0.05$ for all CON *vs.* CR, and genotype comparisons.

Wt and *Ucp3*-KO mitochondria. Surprisingly, CR for 2 wks was without effect on H_2O_2 emission under any of the conditions studied (Table 2).

3.4. Kinetics of H^+ leak in skeletal muscle mitochondria from wild-type and Ucp3-KO mice

The overall kinetics of H^+ leak in skeletal muscle mitochondria from control and CR Wt and *Ucp3*-KO mice are presented in Fig. 2.

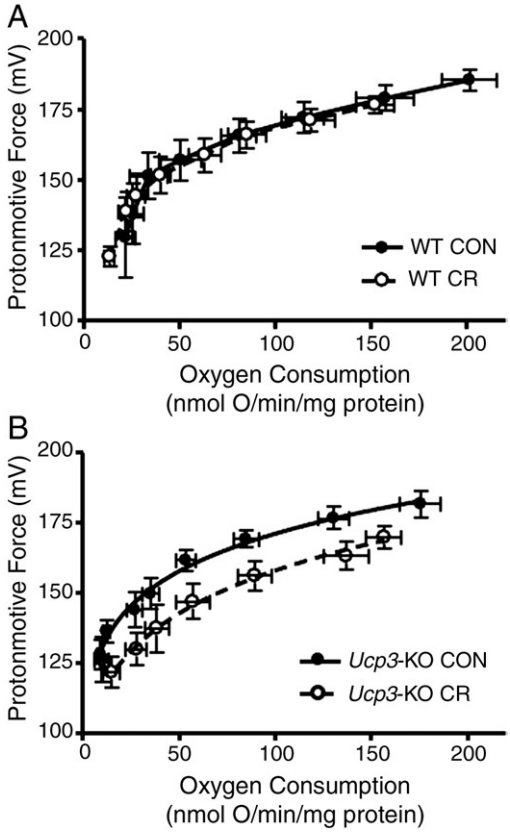

Fig. 2. Increased proton conductance in skeletal muscle mitochondria from *Ucp3*-KO but not Wt mice subjected to 2-wk CR. Leak-dependent respiration and protonmotive force were determined simultaneously using a Clark-type electrode and a $TPMP^+$-selective electrode, respectively. Mitochondria (0.5 mg/ml) were supplied with succinate (10 mM), and determinations were performed in the presence of nigericin (0.4 μg/ml), rotenone (5 μM), oligomycin (8 μg/mg protein), and incremental additions of malonate (0.3–10 mM). Mitochondria from control (CON) and 2-wk CR mice of the same genotype were assayed on any given day; thus data from the Wt (A) and *Ucp3*-KO mice (B) were plotted separately. In each panel, the furthest point on the right represents state 4 respiration. Closed symbols: mitochondria from CON mice; open symbols: mitochondria from CR mice. $N = 6$ mice/group.

Since mitochondria from a control mouse and a CR mouse of the same genotype were tested on the same day, only control and CR data per genotype are plotted together. In mitochondria from Wt mice, maximal H^+ leak-dependent respiration (state 4) was ~24% lower following 2-wk CR ($P<0.05$) whereas state 4 membrane potential was unchanged (Fig. 2A). Proton conductance (*i.e.*, leak-dependent respiration at a given membrane potential) was also unchanged with CR. In mitochondria from *Ucp3*-KO mice, state 4 respiration was unchanged following 2-wk CR whereas maximum achievable membrane potential was 11.9 mV lower ($P<0.05$). Interestingly, and differently from Wt mitochondria, H^+ conductance was increased following CR in *Ucp3*-KO mice (Fig. 2B); when compared at a common membrane potential (170 mV), H^+ leak-dependent O_2 consumption was ~50% greater ($P<0.001$) in mitochondria from *Ucp3*-KO mice subjected to 2-wk CR.

3.5. ANT and UCP3 protein expression

Because ANT has been proposed to mediate ~50% of the basal proton leak [22], we tested the hypothesis that increased protein expression and/or ANT activation was responsible for the greater H^+ conductance in mitochondria from *Ucp3*-KO mice subjected to 2-wk CR. To determine whether the observed differences in H^+ conductance between Wt and *Ucp3*-KO mitochondria (Fig. 2) were due to differences in ANT protein content, we measured ANT protein expression in isolated skeletal muscle mitochondria using an antibody that recognized both the ANT1 and ANT2 isoforms. No differences in ANT protein were detected between any of the genotypes or diet groups (Fig. 3). Two weeks of CR increased UCP3 protein in skeletal muscle mitochondria, as in rats [4,15].

3.6. The ANT activated H^+ leak in skeletal muscle mitochondria from Wt and Ucp3-KO mice

To evaluate the contribution from increased ANT activation, the overall kinetics of H^+ leak was assessed in the presence of CAT, an inhibitor of ANT. These determinations were performed using the same preparations as those described in Fig. 2; thus, the leak curves derived in the absence of CAT are the same in Figs. 2 and 4. Mitochondria from the four groups of mice expressed a CAT-sensitive component of H^+ leak (Fig. 4A – D), although the magnitude of this component was least in mitochondria from control *Ucp3*-KO mice. To further evaluate the CR effect on the CAT-sensitive component of H^+ leak, CAT-sensitive respiration was determined at 170 mV in all groups (Fig. 4E). In mitochondria from Wt mice, CR was without effect on the CAT-sensitive component of H^+ leak. In contrast, the CAT-sensitive component was increased ~3-fold with CR in mitochondria from *Ucp3*-KO mice ($P<0.05$). When the leak curves obtained from control and CR *Ucp3*-KO mitochondria, in the absence and presence of CAT, were plotted together, the curve obtained from CR mouse mitochondria in the presence of CAT is over-imposed on that obtained from control mouse mitochondria obtained in the absence of CAT (Supplemental Fig. 1); thus, the CAT-sensitive conductance entirely accounted for the greater H^+ conductance measured in mitochondria from CR *Ucp3*-KO mice. Differential ANT activation was also evident when BKA was utilized to inhibit ANT (Fig. 4F). Specifically, mitochondria from control *Ucp3*-KO mice exhibited no detectable BKA-sensitive leak whereas a significant BKA-sensitive leak was apparent in mitochondria from *Ucp3*-KO subjected to 2-wk CR.

4. Discussion

Calorie restriction is widely thought to remodel the mitochondrial mass in many tissues including skeletal muscle [4,12–17]. In particular, our previous studies in rats subjected to variable durations of 40% CR (2-wks, 12 and 18 months) demonstrated a rapid and sustained reduction in maximal leak-dependent respiration in skeletal muscle mitochondria [4,15]. This was accompanied by lower mitochondrial ROS generation and oxidative stress and increased UCP3 protein. In skeletal muscle, UCP3 and ANT catalyze various forms of leak-dependent respiration [22,25,29] and

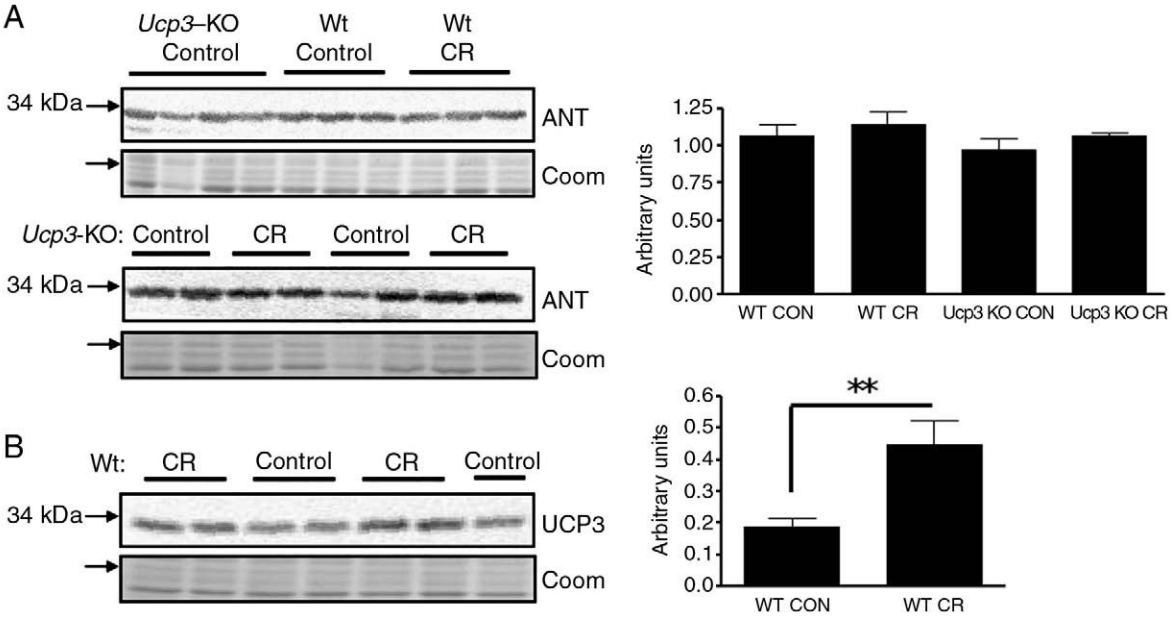

Fig. 3. ANT protein content is unaltered by 2-wk CR in skeletal muscle mitochondria Wt and *Ucp3*-KO mice. Mitochondrial protein (15 μg) from mice subjected to CR and from pair-fed control mice (Control) was probed for ANT (A) and UCP3 (B) protein expression. The antibody raised against ANT recognized both ANT1 and ANT2. Coomassie-stained gels (Coom), shown in grey-scale, served as the loading control. Bar graphs show average expression normalized to the Coomassie loading control, $n=3$–4. ANT protein levels were similar in mitochondria from Wt and *Ucp3*-KO mice, and were unaffected by CR. In contrast, UCP3 protein expression was increased following 2-wk CR (**: $P<0.03$). In A, the same *Ucp3*-KO data are presented in the first and second rows.

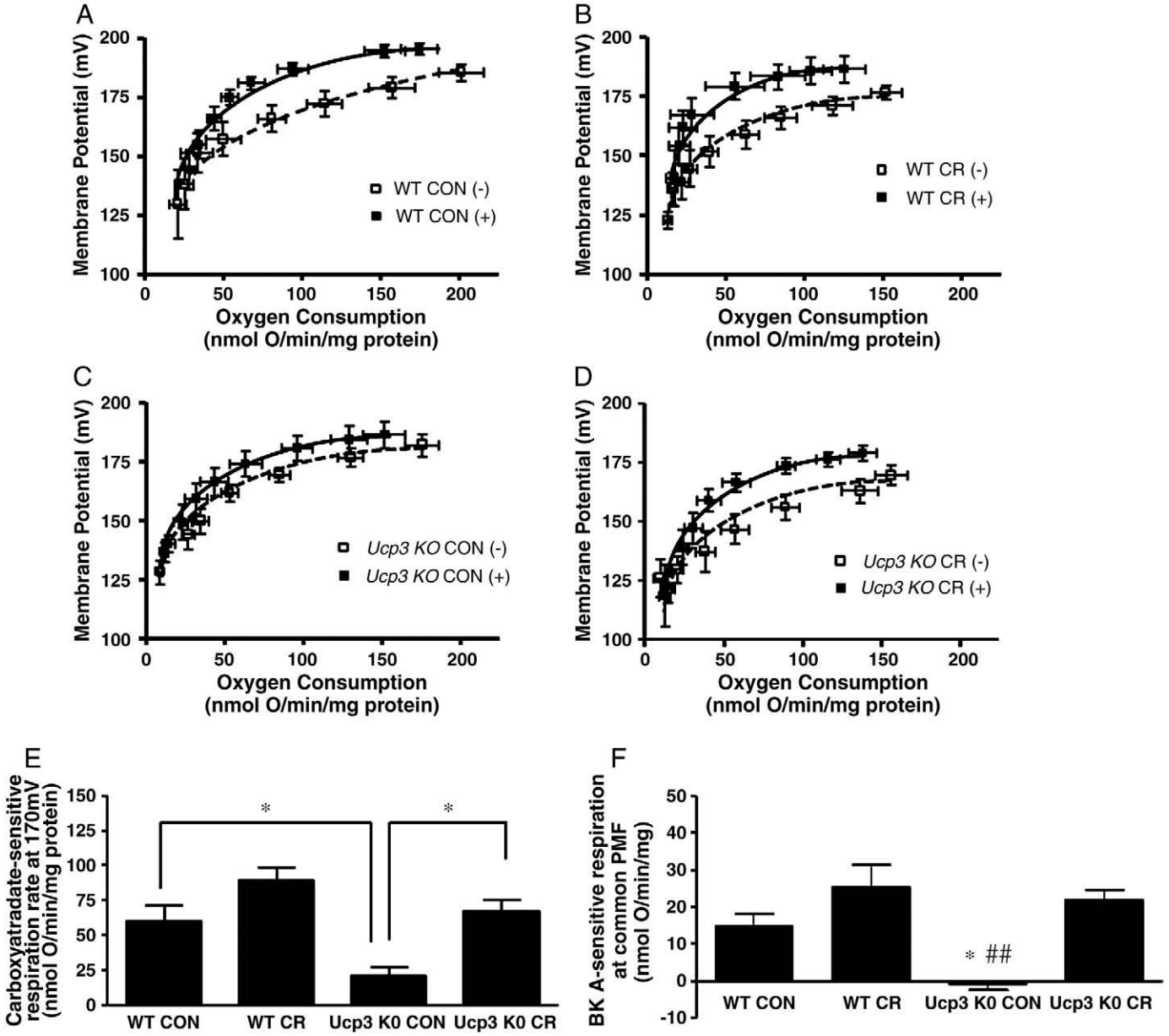

Fig. 4. Increased ANT-sensitive proton leak in skeletal muscle mitochondria from *Ucp3*-KO but not Wt mice subjected to 2-wk CR. Leak-dependent respiration and protonmotive force were determined simultaneously using a Clark-type electrode and a $TPMP^+$-selective electrode, respectively, as described for Fig. 3. Leak curves were determined in the presence (+) and absence (−) of 10 μM carboxyatractylate (CAT). Mitochondria from control (CON) and 2-wk CR mice of the same genotype were assayed on any given day. For clarity, only data with/without CAT per group are plotted on the same graph (panels A – D). Closed symbols: mitochondria from CON mice; open symbols: mitochondria from CR mice. Leak curves generated in the absence of CAT are the same as those presented in Fig. 3. E: The CAT-sensitive respiration rate was determined at a common protonmotive force (170 mV); values are mean ± SEM, $n = 6$ mice/group. *$P<0.05$. F: Experiments depicted in A – D were repeated using bongkrekic acid (BKA; 2 μM) to inhibit ANT, and the BKA-sensitive conductance was calculated at a common protonmotive force (PMF) determined fluorimetrically using safranin (see Experimental procedures); $n = 4$–6; *: $P<0.05$ *vs.* Wt AL, ##: $P<0.01$ *vs.* Wt CR and *Ucp3*-KO CR.

mitigate ROS production [20,28,29]; their role in CR-induced changes in H^+ leak and ROS was investigated here using Wt and *Ucp3*-KO mice. The most important finding is that, in the absence of UCP3, CR leads to greater H^+ conductance possibly mediated by ANT. This observation implies an interaction, or a functional redundancy, between UCP3 and ANT, and suggests that UCP3 can minimize the recruitment of an ANT-mediated 'energy-wasting' process.

4.1. Leak-dependent respiration

Leak-dependent respiration minimizes ROS generation by the electron transport chain [20,48], but is also energetically costly, accounting for ~20% of the basal metabolic rate of rats [49]. Thus, alterations in this functional characteristic could have important consequences in the context of CR. Previously, skeletal muscle mitochondria from rats subjected to 2-wk CR exhibited lower maximal leak-dependent respiration (*i.e.*, state 4) combined with increased H^+ conductance [15]. Here we used *Ucp3*-KO mice together with CAT or BKA to investigate the roles of, respectively, UCP3 and ANT in changes in leak-dependent respiration due to 2-wk CR. In Wt mitochondria, CR was associated with lowered state 4 respiration (Fig. 2A), consistent with our previous findings in rats [15]. Lowered state 4 respiration suggests decreased capacity for H^+ leak. Differently from rats, H^+ leak was unchanged after 2-wk CR; possible explanations for differences in CR effects between rats and mice are discussed below. Mitochondria from *Ucp3*-KO mice responded to CR with unchanged state 4 respiration but a

pronounced increase in H^+ conductance (Fig. 2B). These findings support a role for UCP3 in this aspect of CR-induced mitochondrial remodeling. Specifically, as discussed below, we suggest that UCP3 indirectly modulates H^+ leak through increased ANT activity.

In skeletal muscle mitochondria, ~50% of the H^+ leak is attributable to ANT, much of it not inhibited by CAT, and thus is not due to ADP/ATP exchange or activation by, *e.g.*, fatty acids [22]; this CAT-insensitive component is termed 'basal' [22]. ANT can also catalyze a CAT-inhibited 'activated' H^+ leak; activators are fatty acids [22–25], alkenals [26] and AMP [27]. We hypothesized that the greater H^+ conductance in mitochondria from *Ucp3*-KO CR mice reflected higher ANT content and/or activation, and thus assessed ANT protein levels and the CAT-sensitive leak. ANT protein expression was similar in mitochondria from control Wt and *Ucp3*-KO mice, and was unaltered by CR in either genotype. In contrast, a CAT-sensitive leak was measurable in both genotypes, whether control or CR, but was significantly increased with CR in *Ucp3*-KO mitochondria only (Fig. 4E). Use of BKA to inhibit ANT revealed a BKA-sensitive conductance in mitochondria from both Wt groups but only from 2-wk CR *Ucp3*-KO mice. Thus, the increased H^+ conductance in mitochondria from *Ucp3*-KO CR mice may be explained by greater ANT activation. This conclusion, however, needs to be interpreted in light of observations that CAT or BKA can indirectly inhibit UCP3 via ANT [36]. In particular, the inhibition of proton leak by CAT and GDP (which can inhibit UCPs) is not additive. Specifically, these investigators showed that inhibition of H^+ conductance by CAT+GDP is similar to that by CAT alone whereas inhibition by GDP is lower (*i.e.*, the GDP-sensitive conductance is lower), suggesting that CAT inhibits the conductance mediated by both ANT and UCP3 [26,36]. Thus, it is perhaps not surprising that we observed greater CAT- and BKA-sensitive conductances in mitochondria from Wt control as compared to *Ucp3*-KO control mice. Moreover, the trend for greater CAT- and BKA-sensitive conductances with CR in Wt mitochondria is consistent with the higher levels of UCP3 protein following CR (Fig. 3). In contrast, CAT- and BKA-sensitive conductances were strikingly elevated in mitochondria from *Ucp3*-KO CR mice, and this occurred in the absence of an increase in ANT (or UCP3) protein. Thus it seems that ANT was more greatly activated in mitochondria from *Ucp3*-KO but not from Wt mice subjected to CR. Moreover, that the CAT-inhibited leak curve in mitochondria from *Ucp3*-KO CR mice could be superimposed on the curves from Wt control and CR mitochondria (Suppl. Fig. 1), suggests that the elevated H^+ conductance in mitochondria from *Ucp3*-KO CR mice was due entirely to greater ANT activation. The ANT1 isoform, which is highly expressed in skeletal and cardiac muscle, may mediate basal leak whereas the ubiquitously expressed ANT2 isoform may mediate inducible leak [25]. Thus, increased activation of ANT2 was likely responsible for the greater CAT-sensitive leak in mitochondria from CR *Ucp3*-KO mice.

We have found that GDP can partially inhibit H^+ leak, but to the same extent in Wt and *Ucp3*-KO mitochondria, even in incubation medium devoid of Mg^{2+} [Seifert, Estey, Harper; unpublished observations], as reported by Brand's group [36]. Thus, GDP was not useful in our hands for analysis of UCP3-specific activation. Similarly, as discussed above, interpretation of results obtained with CAT and BKA could be confounded in Wt mitochondria by an indirect effect of the inhibitors on UCP3. However, use of CAT or BKA in *Ucp3*-KO mitochondria would not be complicated in this way. Another point is whether ANT (and UCP3) are activated under the conditions of our experiments, namely with albumin (0.3%) and Mg^{2+} present in the incubation medium which would, respectively, bind endogenous fatty acids [36] and inhibit leak-dependent respiration [27]. However, expression of a CAT-sensitive conductance under these conditions [present study, [22,25,36]] clearly demonstrates that ANT activation occurs. UCP3 activation under similar conditions has also been demonstrated [36,50].

4.2. ROS production

CR has been associated with lowered oxidative stress [3–5,15,17], consistent with the oxidative stress theory of aging. Because UCP3 is functionally and mechanistically linked to decreased oxidative stress (for review: [28,29]), it was of interest to determine whether UCP3 contributes to the CR-induced lowering of oxidative stress. Surprisingly, ROS formation (measured as H_2O_2 emission) in skeletal muscle mitochondria was unaltered by 2-wk CR in mice of both genotypes. Unchanged H_2O_2 emission with CR was despite an extensive assessment of ROS formation at different sites in the mitochondrial electron transport chain. Mitochondrial ROS generation was however lower in mice when CR was extended to 1 month [Estey et al., in preparation]. CR lasting >1 month was also associated with decreased oxidative stress in mouse skeletal muscle [3,5]. Differently from mice, rats subjected to 2-wk CR showed lower ROS generation and oxidative stress in muscle mitochondria [15]. H_2O_2 emission was determined by the same technique in the latter study [15] as in the present one, ruling out a methodological explanation for the species difference. Thus, CR is not unequivocally associated with lowered ROS production oxidative stress, in agreement with findings from rat hepatocytes [51]. The mechanistic basis for the species difference in the short-term CR effect on ROS is unknown. Fiber type differences in ROS production have been reported [52]. Yet, it seems unlikely that a fiber type bias would explain the difference between mice and rats because mitochondria from both species were isolated from muscle groups containing primarily type II fibers that include both IIa (more aerobic) and IIb (highly glycolytic) fibers. Overall, our observations indicate that CR effects in one species cannot necessarily be extrapolated to another.

Because the 2-wk CR intervention in mice did not result in changed ROS generation in muscle mitochondria, we cannot make definitive statements regarding the role of UCP3 to alter ROS in the context of CR. Interestingly, UCP3 protein increased with 2-wk CR in mice (present study) and rats [15] whereas H_2O_2 emission rate was reduced only in rats. On the surface this suggests that UCP3 is not important for mitigating oxidative stress. However, the mitochondrial ROS load is a complex function of the anti-oxidant capacity, the mix of substrates being oxidized, and the extent of membrane energization. The latter depends upon ATP demand as well as the functional mitochondrial mass (although neither of these factors is relevant in isolated mitochondria). CR could potentially alter each of the above-mentioned processes and characteristics; yet, little is known about the impact of CR on many of these variables in skeletal muscle, an issue that is also relevant to the species difference in the CR effect on ROS. Possibly, UCP3 offsets a greater capacity for ROS formation with 2-wk CR due to lowered leak-dependent respiration [this study, [4,15]] and/or increased fatty acid oxidation. If UCP3 plays such a role, our observations suggest that ANT activity can increase to compensate for the lack of UCP3.

Although not the focus here, it is noteworthy that we failed to detect a difference in H_2O_2 emission in mitochondria from control Wt and *Ucp3*-KO mice, consistent with our previous findings from mitochondria supplied with palmitoylcarnitine+antimycin+SOD [53]. The present study extends this analysis to other sites of ROS production. Using permeabilized muscle fibers supplied with succinate, Anderson et al. also failed to detect a difference in H_2O_2 emission in *Ucp3*-KO muscle [52]. MnSOD2 protein is not elevated in muscle from our *Ucp3*-KO mice, whether fed or fasted, and UCP2 protein is not expressed [53]. Higher H_2O_2 emission was however detected in muscle mitochondria from fasted or exercise-trained *Ucp3*-KO mice [52] [53], interventions that normally increase UCP3 protein. Both interventions also increase fatty acid oxidation (FAO) and thus would be associated with greater mitochondrial lipid peroxidation and reactive alkenals generation. Although the latter could explain increased oxidative stress in mitochondria from fasted or exercise-trained *Ucp3*-KO mice, it would

not explain greater H_2O_2 emission in isolated mitochondria. Possibly, increased FAO, as occurs with CR, is associated with altered phospholipid composition of the mitochondrial inner membrane such that more reactive or abundant lipid peroxidation products are generated leading to greater activation of UCP3. Clearly, the link between UCP3 and lower oxidative stress requires further investigation.

4.3. Whole-body energetics and organ weights

Whole-body VO_2 was reduced with CR when measurements were expressed per mouse; this difference disappeared when VO_2 values were adjusted for BW, as is common practice. The conclusion that whole-body VO_2 was unaffected by CR would, however, be erroneous because body composition changes with CR [54,55]. In fact, CR decreased the proportion of fat mass while having little effect on the proportion of lean tissue mass. Consequently, CR mice contained more metabolically active tissue per BW than control mice, indicating that that whole-body VO_2 was lowered by 2-wk CR. CR-induced changes in whole-body VO_2 and body and organ weights were similar in Wt and *Ucp3*-KO mice. In addition, *Ucp3*-KO mice, like Wt mice, lowered RER in response to CR, and to the same extent, indicating a similar rise in FAO. This observation appears to conflict with findings that link UCP3 with increased FAO [53,56,57]. However, indirect calorimetry may not be sensitive enough to detect small changes in FAO or coupling efficiency of muscle mitochondria from CR *Ucp3*-KO mice. Future studies utilizing localized measurements of muscle energetics *in vivo* [58] could address whether the latter are altered due to UCP3 absence.

In summary, absence of UCP3 is associated with increased H^+ conductance in skeletal muscle mitochondria of mice subjected to 2-wks CR, implicating UCP3 in CR-induced mitochondrial remodeling. Results reveal that the greater H^+ conductance is due to increased ANT activation. Thus UCP3 may curtail recruitment of an ANT-mediated energy consuming process. The present study does not identify the cause of the greater ANT activation. Possibilities are: 1) greater ANT activation despite similar types and levels of endogenous stimuli as in Wt mitochondria; 2) greater activation due to increased abundance of activator(s) in mitochondria from *Ucp3*-KO CR mice. The first possibility implies a physical interaction between UCP3 and ANT. The second implies a functional compensation by ANT for UCP3. Future experiments should be designed to test these alternatives.

Acknowledgements

This research was funded through an operating grant from the Canadian Institutes of Health Research: Institute of Nutrition, Metabolism and Diabetes (#57810). LB was supported by a scholarship from NSERC. ELS was supported by a fellowship from the Canadian Diabetes Association.

Appendix A. Supplementary data

Supplementary data associated with this article can be found, in the online version, at doi:10.1016/j.bbabio.2010.02.018.

References

[1] R.M. Anderson, D. Shanmuganayagam, R. Weindruch, Caloric restriction and aging: studies in mice and monkeys, Toxicol. Pathol. 37 (2009) 47–51.
[2] L.K. Heilbronn, L. de Jonge, M.I. Frisard, J.P. DeLany, D.E. Larson-Meyer, J. Rood, T. Nguyen, C.K. Martin, J. Volaufova, M.M. Most, F.L. Greenway, S.R. Smith, W.A. Deutsch, D.A. Williamson, E. Ravussin, Effect of 6-month calorie restriction on biomarkers of longevity, metabolic adaptation, and oxidative stress in overweight individuals: a randomized controlled trial, JAMA 295 (2006) 1539–1548.
[3] D.K. Asami, R.B. McDonald, K. Hagopian, B.A. Horwitz, D. Warman, A. Hsiao, C. Warden, J.J. Ramsey, Effect of aging, caloric restriction, and uncoupling protein 3 (UCP3) on mitochondrial proton leak in mice, Exp. Gerontol. 43 (2008) 1069–1076.
[4] L. Bevilacqua, J.J. Ramsey, K. Hagopian, R. Weindruch, M.E. Harper, Long-term caloric restriction increases UCP3 content but decreases proton leak and reactive oxygen species production in rat skeletal muscle mitochondria, Am. J. Physiol. Endocrinol. Metab. 289 (2005) E429–E438.
[5] A. Lass, B.H. Sohal, R. Weindruch, M.J. Forster, R.S. Sohal, Caloric restriction prevents age-associated accrual of oxidative damage to mouse skeletal muscle mitochondria, Free Radic. Biol. Med. 25 (1998) 1089–1097.
[6] D. Harman, Aging: a theory based on free radical and radiation chemistry, J. Gerontol. 11 (1956) 298–300.
[7] D. Harman, Free radical theory of aging: dietary implications, Am. J. Clin. Nutr. 25 (1972) 839–843.
[8] R.S. Sohal, R. Weindruch, Oxidative stress, caloric restriction, and aging, Science 273 (1996) 59–63.
[9] B. Chance, H. Sies, A. Boveris, Hydroperoxide metabolism in mammalian organs, Physiol. Rev. 59 (1979) 527–605.
[10] R.G. Hansford, B.A. Hogue, V. Mildaziene, Dependence of H2O2 formation by rat heart mitochondria on substrate availability and donor age, J. Bioenerg. Biomembr. 29 (1997) 89–95.
[11] L. Guarente, Mitochondria—a nexus for aging, calorie restriction, and sirtuins? Cell 132 (2008) 171–176.
[12] E. Marzetti, J.M. Lawler, A. Hiona, T. Manini, A.Y. Seo, C. Leeuwenburgh, Modulation of age-induced apoptotic signaling and cellular remodeling by exercise and calorie restriction in skeletal muscle, Free Radic. Biol. Med. 44 (2008) 160–168.
[13] A.E. Civitarese, S. Carling, L.K. Heilbronn, M.H. Hulver, B. Ukropcova, W.A. Deutsch, S.R. Smith, E. Ravussin, Calorie restriction increases muscle mitochondrial biogenesis in healthy humans, PLoS Med. 4 (2007) e76.
[14] R. Barazzoni, M. Zanetti, A. Bosutti, G. Biolo, L. Vitali-Serdoz, M. Stebel, G. Guarnieri, Moderate caloric restriction, but not physiological hyperleptinemia per se, enhances mitochondrial oxidative capacity in rat liver and skeletal muscle-tissue-specific impact on tissue triglyceride content and AKT activation, Endocrinology 146 (2005) 2098–2106.
[15] L. Bevilacqua, J.J. Ramsey, K. Hagopian, R. Weindruch, M.E. Harper, Effects of short- and medium-term calorie restriction on muscle mitochondrial proton leak and reactive oxygen species production, Am. J. Physiol. Endocrinol. Metab. 286 (2004) E852–E861.
[16] E. Bua, S.H. McKiernan, J.M. Aiken, Calorie restriction limits the generation but not the progression of mitochondrial abnormalities in aging skeletal muscle, FASEB J. 18 (2004) 582–584.
[17] R. Pamplona, M. Portero-Otin, J. Requena, R. Gredilla, G. Barja, Oxidative, glycoxidative and lipoxidative damage to rat heart mitochondrial proteins is lower after 4 months of caloric restriction than in age-matched controls, Mech. Ageing Dev. 123 (2002) 1437–1446.
[18] C.E. Amara, E.G. Shankland, S.A. Jubrias, D.J. Marcinek, M.J. Kushmerick, K.E. Conley, Mild mitochondrial uncoupling impacts cellular aging in human muscles in vivo, Proc. Natl. Acad. Sci. U. S. A. 104 (2007) 1057–1062.
[19] M.D. Brand, L.F. Chien, E.K. Ainscow, D.F. Rolfe, R.K. Porter, The causes and functions of mitochondrial proton leak, Biochim. Biophys. Acta 1187 (1994) 132–139.
[20] V.P. Skulachev, Uncoupling: new approaches to an old problem of bioenergetics, Biochim. Biophys. Acta 1363 (1998) 100–124.
[21] M.E. Harper, K. Green, M.D. Brand, The efficiency of cellular energy transduction and its implications for obesity, Annu. Rev. Nutr. 28 (2008) 13–33.
[22] M.D. Brand, J.L. Pakay, A. Ocloo, J. Kokoszka, D.C. Wallace, P.S. Brookes, E.J. Cornwall, The basal proton conductance of mitochondria depends on adenine nucleotide translocase content, Biochem. J. 392 (2005) 353–362.
[23] A. Andreyev, T.O. Bondareva, V.I. Dedukhova, E.N. Mokhova, V.P. Skulachev, N.I. Volkov, Carboxyatractylate inhibits the uncoupling effect of free fatty acids, FEBS Lett. 226 (1988) 265–269.
[24] A. Andreyev, T.O. Bondareva, V.I. Dedukhova, E.N. Mokhova, V.P. Skulachev, L.M. Tsofina, N.I. Volkov, T.V. Vygodina, The ATP/ADP-antiporter is involved in the uncoupling effect of fatty acids on mitochondria, Eur. J. Biochem. 182 (1989) 585–592.
[25] I.G. Shabalina, T.V. Kramarova, J. Nedergaard, B. Cannon, Carboxyatractyloside effects on brown-fat mitochondria imply that the adenine nucleotide translocator isoforms ANT1 and ANT2 may be responsible for basal and fatty-acid-induced uncoupling respectively, Biochem. J. 399 (2006) 405–414.
[26] K.S. Echtay, T.C. Esteves, J.L. Pakay, M.B. Jekabsons, A.J. Lambert, M. Portero-Otin, R. Pamplona, A.J. Vidal-Puig, S. Wang, S.J. Roebuck, M.D. Brand, A signalling role for 4-hydroxy-2-nonenal in regulation of mitochondrial uncoupling, EMBO J. 22 (2003) 4103–4110.
[27] S. Cadenas, J.A. Buckingham, J. St-Pierre, K. Dickinson, R.B. Jones, M.D. Brand, AMP decreases the efficiency of skeletal-muscle mitochondria, Biochem. J. 351 (Pt 2) (2000) 307–311.
[28] M.D. Brand, T.C. Esteves, Physiological functions of the mitochondrial uncoupling proteins UCP2 and UCP3, Cell Metab. 2 (2005) 85–93.
[29] V. Bezaire, E.L. Seifert, M.E. Harper, Uncoupling protein-3: clues in an ongoing mitochondrial mystery, FASEB J. 21 (2007) 312–324.
[30] M. Riachi, J. Himms-Hagen, M.E. Harper, Percent relative cumulative frequency analysis in indirect calorimetry: application to studies of transgenic mice, Can. J. Physiol. Pharmacol. 82 (2004) 1075–1083.
[31] J.B. Chappell, S.V. Perry, Biochemical and osmotic properties of skeletal muscle mitochondria, Nature 173 (1954) 1094–1095.
[32] M.W. Makinen, C.P. Lee, G.M. Shy, Microanalysis of cytochrome content, oxidative and phosphorylative activities of human skeletal muscle mitochondria, Neurology 18 (1968) 299.
[33] N. Kamo, M. Muratsugu, R. Hongoh, Y. Kobatake, Membrane potential of mitochondria measured with an electrode sensitive to tetraphenyl phosphonium

and relationship between proton electrochemical potential and phosphorylation potential in steady state, J. Membr. Biol. 49 (1979) 105–121.
[34] J.J. Ramsey, K. Hagopian, T.M. Kenny, E.K. Koomson, L. Bevilacqua, R. Weindruch, M. E. Harper, Proton leak and hydrogen peroxide production in liver mitochondria from energy-restricted rats, Am. J. Physiol. Endocrinol. Metab. 286 (2004) E31–E40.
[35] K.E. Akerman, M.K. Wikstrom, Safranine as a probe of the mitochondrial membrane potential, FEBS Lett. 68 (1976) 191–197.
[36] N. Parker, C. Affourtit, A. Vidal-Puig, M.D. Brand, Energization-dependent endogenous activation of proton conductance in skeletal muscle mitochondria, Biochem. J. 412 (2008) 131–139.
[37] S. Cadenas, M.D. Brand, Effects of magnesium and nucleotides on the proton conductance of rat skeletal-muscle mitochondria, Biochem. J. 348 (Pt 1) (2000) 209–213.
[38] M. Klingenberg, M. Buchholz, On the mechanism of bongkrekate effect on the mitochondrial adenine-nucleotide carrier as studied through the binding of ADP, Eur. J. Biochem. 38 (1973) 346–358.
[39] P.A. Hyslop, L.A. Sklar, A quantitative fluorimetric assay for the determination of oxidant production by polymorphonuclear leukocytes: its use in the simultaneous fluorimetric assay of cellular activation processes, Anal. Biochem. 141 (1984) 280–286.
[40] V. Bezaire, W. Hofmann, J.K. Kramer, L.P. Kozak, M.E. Harper, Effects of fasting on muscle mitochondrial energetics and fatty acid metabolism in Ucp3(−/−) and wild-type mice, Am. J. Physiol. Endocrinol. Metab. 281 (2001) E975–E982.
[41] D.W. Gong, S. Monemdjou, O. Gavrilova, L.R. Leon, B. Marcus-Samuels, C.J. Chou, C. Everett, L.P. Kozak, C. Li, C. Deng, M.E. Harper, M.L. Reitman, Lack of obesity and normal response to fasting and thyroid hormone in mice lacking uncoupling protein-3, J. Biol. Chem. 275 (2000) 16251–16257.
[42] S.C. Faulks, N. Turner, P.L. Else, A.J. Hulbert, Calorie restriction in mice: effects on body composition, daily activity, metabolic rate, mitochondrial reactive oxygen species production, and membrane fatty acid composition, J. Gerontol. A Biol. Sci. Med. Sci. 61 (2006) 781–794.
[43] R.J. Colman, R.M. Anderson, S.C. Johnson, E.K. Kastman, K.J. Kosmatka, T.M. Beasley, D.B. Allison, C. Cruzen, H.A. Simmons, J.W. Kemnitz, R. Weindruch, Caloric restriction delays disease onset and mortality in rhesus monkeys, Science 325 (2009) 201–204.
[44] A.A. Starkov, G. Fiskum, C. Chinopoulos, B.J. Lorenzo, S.E. Browne, M.S. Patel, M.F. Beal, Mitochondrial alpha-ketoglutarate dehydrogenase complex generates reactive oxygen species, J. Neurosci. 24 (2004) 7779–7788.
[45] J. St-Pierre, J.A. Buckingham, S.J. Roebuck, M.D. Brand, Topology of superoxide production from different sites in the mitochondrial electron transport chain, J. Biol. Chem. 277 (2002) 44784–44790.
[46] E.L. Seifert, C. Estey, J.Y. Xuan, M.E. Harper, Electron transport chain dependent and independent mechanisms of mitochondrial H2O2 emission during long-chain fatty acid oxidation, J. Biol. Chem. 285 (2010) 5748–5758.
[47] Y. Liu, G. Fiskum, D. Schubert, Generation of reactive oxygen species by the mitochondrial electron transport chain, J. Neurochem. 80 (2002) 780–787.
[48] S.S. Korshunov, V.P. Skulachev, A.A. Starkov, High protonic potential actuates a mechanism of production of reactive oxygen species in mitochondria, FEBS Lett. 416 (1997) 15–18.
[49] D.F. Rolfe, J.M. Newman, J.A. Buckingham, M.G. Clark, M.D. Brand, Contribution of mitochondrial proton leak to respiration rate in working skeletal muscle and liver and to SMR, Am. J. Physiol. 276 (1999) C692–C699.
[50] D.A. Talbot, M.D. Brand, Uncoupling protein 3 protects aconitase against inactivation in isolated skeletal muscle mitochondria, Biochim. Biophys. Acta 1709 (2005) 150–156.
[51] A.J. Lambert, B.J. Merry, Lack of effect of caloric restriction on bioenergetics and reactive oxygen species production in intact rat hepatocytes, J. Gerontol. A Biol. Sci. Med. Sci. 60 (2005) 175–180.
[52] E.J. Anderson, H. Yamazaki, P.D. Neufer, Induction of endogenous uncoupling protein 3 suppresses mitochondrial oxidant emission during fatty acid-supported respiration, J. Biol. Chem. 282 (2007) 31257–31266.
[53] E.L. Seifert, V. Bezaire, C. Estey, M.E. Harper, Essential role for uncoupling protein-3 in mitochondrial adaptation to fasting but not in fatty acid oxidation or fatty acid anion export, J. Biol. Chem. 283 (2008) 25124–25131.
[54] J. Himms-Hagen, On raising energy expenditure in ob/ob mice, Science 276 (1997) 1132–1133.
[55] J.J. Ramsey, M.E. Harper, R. Weindruch, Restriction of energy intake, energy expenditure, and aging, Free Radic. Biol. Med. 29 (2000) 946–968.
[56] S. Samec, J. Seydoux, A.G. Dulloo, Role of UCP homologues in skeletal muscles and brown adipose tissue: mediators of thermogenesis or regulators of lipids as fuel substrate? FASEB J. 12 (1998) 715–724.
[57] J.D. MacLellan, M.F. Gerrits, A. Gowing, P.J. Smith, M.B. Wheeler, M.E. Harper, Physiological increases in uncoupling protein 3 augment fatty acid oxidation and decrease reactive oxygen species production without uncoupling respiration in muscle cells, Diabetes 54 (2005) 2343–2350.
[58] D.J. Marcinek, K.A. Schenkman, W.A. Ciesielski, K.E. Conley, Mitochondrial coupling in vivo in mouse skeletal muscle, Am. J. Physiol. Cell Physiol 286 (2004) C457–C463.